Organometallics 1994, *13*, 141–147

Coordination of Sulfur Dioxide to Iridium(I) Centers. Sulfur Dioxide Insertion into a Methoxo–Metal Bond: Crystal and Molecular Structure of Carbonyl(methyl sulfito)(sulfur dioxide)bis(triphenylphosphine)iridium–Hemitoluene, the First Structurally Characterized Example of a Transition Metal Complex Containing an O-Coordinated Methyl Sulfito Ligand

Sherri L. Randall, Cynthia A. Miller, Thomas S. Janik,[†]
Melvyn Rowen Churchill,* and Jim D. Atwood*

Department of Chemistry, University at Buffalo, State University of New York at Buffalo, Buffalo, New York 14214

Received August 3, 1993[●]

Reactions of SO_2 with iridium(I) complexes have been examined. For *trans*-$Ir(CO)L_2X$ (L = PPh_3, $P(p\text{-tolyl})_3$, PCy_3; X = Cl, Br, Me), equilibrium constants for SO_2 binding have been evaluated. The binding of SO_2 is as a Lewis acid and is enhanced by electron-donating groups on the iridium. Increasing the size of the phosphine reduces the equilibrium constant for SO_2 binding. Reactions of SO_2 with the hydroxo or alkoxo complexes $Ir(CO)(OR)L_2$ (R = H, Me, *t*-Bu; L = PPh_3, $P(p\text{-tolyl})_3$) result in insertion of the SO_2 to form an oxygen-coordinated sulfite ligand. The sulfur center of the sulfite ligand is pyramidal and asymmetric, resulting in a second-order ^{31}P NMR spectrum at low temperature. A further rearrangement of the oxygen-coordinated sulfite ligand to the sulfur-coordinated occurs in solution. For R = H, further decomposition of the HSO_3^- ligand occurs. The products of each reaction are characterized by infrared and ^1H and ^{31}P NMR spectroscopy. The product of SO_2 insertion into the iridium–methoxo bond, $Ir(CO)(OS(O)OMe)(SO_2)(PPh_3)_2$, is also characterized by X-ray crystallography. The complex $Ir(CO)[OS(O)OMe](SO_2)(PPh_3)_2$ crystallizes from toluene as the hemitoluene solvate, $Ir(CO)[OS(O)OMe](SO_2)(PPh_3)_2\cdot 0.5$(toluene), in the centrosymmetric triclinic space group $P\bar{1}$ (No. 2) with a = 10.972(5) Å, b = 11.658(4) Å, c = 18.020(11) Å, α = 82.73(4)°, β = 77.76(4)°, γ = 63.25(3)°, V = 2007.5(17) Å^3, and Z = 2. The structure was solved and refined to R = 3.05% and R_w = 3.58% for all 5280 reflections with $2\theta < 45°$ (Mo Kα) and R = 2.31% and R_w = 3.23% for those 4502 reflections with $|F_o| > 6\sigma(F_o)$. The iridium is in a square-pyramidal coordination environment with the SO_2 ligand in the apical site. Iridium–ligand bond lengths are as follows: Ir(1)–P(1) = 2.369(2) Å and Ir(1)–P(2) = 2.387(2) Å for the Ir–PPh_3 groups, Ir(1)–S(1) = 2.451(2) Å for the SO_2 ligand, Ir(1)–C(1) = 1.831(6) Å for the CO ligand, and Ir–O(23) = 2.080(4) Å for the OS(=O)OMe ligand. The trans-basal angles are P(1)–Ir(1)–P(2) = 170.3(1)° and C(1)–Ir(1)–O(23) = 176.7(2)°; angles to the apical SO_2 ligand are P(1)–Ir(1)–S(1) = 97.5(1)°, P(2)–Ir(1)–S(1) = 92.2(1)°, C(1)–Ir(1)–S(1) = 97.3(2)°, and O(23)–Ir(1)–S(1) = 85.8(1)°.

The coordination chemistry of SO_2 is reasonably well understood, with eight different coordination modes observed.[1,2] Kubas has provided the most recent investigations, aimed primarily at reduction of SO_2,[2-7] with a catalytic cycle reported for reduction of SO_2 to S and H_2O.[7] Reactions of SO_2 with transition metal hydrides have given several types of products, including those with insertion of SO_2 into the metal hydride. Reaction of SO_2 with $Cp^*Ru(CO)_2H$ illustrates one type of product formation.[3,4]

$$Cp^*Ru(CO)_2H + SO_2 \rightarrow Cp^*Ru(CO)_2SO_3H + [Cp^*Ru(CO)_2]_2(\mu\text{-}S_2O_3) \quad (1)$$

Another study has shown oxidation of a bridging SO_2 to a bridging SO_3.[8]

$$2Pt(cod)_2 + 2SO_2 \rightarrow [Pt(cod)_2]_2(\mu\text{-}SO_2)_2 \xrightarrow{O_2} [Pt(cod)_2]_2(\mu\text{-}SO_3)(\mu\text{-}SO_2) \quad (2)$$

In the bridged products, one of the cod (cod = cyclooctadiene) double bonds is no longer coordinated.[8]

[†] Permanent address: Department of Chemistry, State University College at Fredonia, Fredonia, NY.

[●] Abstract published in *Advance ACS Abstracts*, November 15, 1993.

(1) Schenk, W. A. *Angew. Chem., Int. Ed. Engl.* **1987**, *26*, 98.

(2) (a) Kubas, G. J. *Inorg. Chem.* **1979**, *18*, 182 and references therein. (b) Ryan, R. R.; Kubas, G. J.; Moody, D. C.; Eller, P. G. *Struct. Bonding* **1981**, *46*, 48.

(3) Kubat-Martin, K. A.; Kubas, G. J.; Ryan, R. R. *Organometallics* **1989**, *8*, 1910.

(4) Kubat-Martin, K. A.; Kubas, G. J.; Ryan, R. R. *Organometallics* **1988**, *7*, 1657.

(5) Kubas, G. J.; Wasserman, H. J.; Ryan, R. R. *Organometallics* **1985**, *4*, 2012.

(6) Kubas, G. J.; Ryan, R. R. *J. Am. Chem. Soc.* **1985**, *107*, 6138.

(7) Kubas, G. J.; Ryan, R. R. *Polyhedron* **1986**, *5*, 473.

(8) Farrar, D. H.; Gukathasan, R. R. *J. Chem. Soc., Dalton Trans.* **1989**, 557.

0276-7333/94/2313-0141$04.50/0

Iridium complexes with SO_2 have also been reported.[9-13] Vaska's complex forms a simple adduct, $Ir(CO)(Cl)(SO_2)(PPh_3)_2$:

$$\textit{trans}\text{-}\mathrm{Ir(CO)(Cl)(PPh_3)_2 + SO_2 \rightleftarrows Ir(CO)(Cl)(SO_2)(PPh_3)_2} \quad (3)$$

The structure has been determined,[10] and an equilibrium constant has been evaluated.[11] The possibility of using absorption of SO_2 by solid $Ir(CO)(PPh_3)_2Cl$ to remove SO_2 from flue gases has been reported.[14] It is also possible to prepare the hydrido analogue by displacement of PPh_3 from $Ir(CO)(H)(PPh_3)_3$.[12,13]

$$\mathrm{Ir(CO)(H)(PPh_3)_3 + SO_2 \rightarrow Ir(CO)(H)(SO_2)(PPh_3)_2 + PPh_3} \quad (4)$$

A tautomerism involving SO_2 insertion into the Ir–H bond was suggested.[13] In other cases, the reaction of iridium complexes *trans*-$Ir(CO)(X)(L)_2$ with a combination of SO_2 and O_2 leads to bidentate sulfate complexes.[9,15,16]

$$\mathrm{Ir(CO)(X)L_2 + SO_2/O_2 \rightarrow Ir(CO)(X)(SO_4)L_2} \quad (5)$$

$$\mathrm{X = Cl, Me;\ L = PPh_3, P(}p\mathrm{\text{-}tolyl)_3}$$

In this paper, further studies of SO_2 binding to iridium(I) are described. Ligand effects on the equilibrium constant for SO_2 binding are evaluated, and the formation of an oxygen-coordinated methyl sulfito ligand from insertion of SO_2 into an Ir–OMe bond is described.

Experimental Section

Materials. $IrCl_3{\cdot}3H_2O$ was purchased or borrowed from Johnson Matthey. Triphenylphosphine and tri-*p*-tolylphosphine were purchased from Strem Chemical Co. Gases (SO_2, O_2, and gas mixtures: 958 ppm of SO_2 in N_2, 1.06% SO_2 in N_2, 9.73% SO_2 in N_2, 103 ppm of SO_2 in air, 936 ppm of SO_2 in air, and 1.1% SO_2 in air) were purchased from Matheson. Methyllithium was purchased from Aldrich Chemical Co. or Lithco, Inc. All of these materials were used as received without further purification.

Solvents. Benzene, toluene, THF, and diethyl ether were refluxed in a N_2 atmosphere over Na/benzophenone until the solutions became blue or purple. Cyclohexane and acetonitrile were refluxed in a N_2 atmosphere with finely divided CaH_2 overnight. The solvent was then distilled into a collection flask which had been evacuated three times with subsequent N_2 backfilling. The purified solvents were stored in an inert-atmosphere glovebox.

All deuterated solvents (CD_2Cl_2, C_6D_6, C_7D_8) were stirred overnight with finely divided CaH_2, followed by vacuum distillation into an oven-dried pressure tube fitted with a Teflon stopcock. The purified solvents were stored in an inert-atmosphere glovebox. Deuterated solvents were purchased from Cambridge Isotope Labs, Aldrich, or MSD Isotopes.

Instrumental Measurements. ^1H and ^{31}P NMR spectra were recorded on a Varian VXR-400. References were set to residual solvent peaks in ^1H NMR spectra. ^{31}P NMR spectra were referenced to an external sample of H_3PO_4 at 0.0 ppm and are proton decoupled unless otherwise noted. All chemical shifts are reported in ppm, and all coupling constants (J) are reported in Hz. Infrared spectra were obtained using a Mattson Polaris Fourier transform spectrometer with 0.5-mm NaCl solution cells or as KBr disks.

Preparations. All syntheses were accomplished under an argon or nitrogen atmosphere (unless otherwise noted) using an argon-filled glovebox, Schlenk techniques, or high-vacuum techniques. Square planar iridium complexes, *trans*-$Ir(CO)(Cl)[P(p\text{-tolyl})_3]_2$, *trans*-$Ir(CO)(OH)[P(p\text{-tolyl})_3]_2$, *trans*-$Ir(CO)(OH)(PPh_3)_2$, *trans*-$Ir(CO)(Me)[P(p\text{-tolyl})_3]_2$, *trans*-$Ir(CO)(OMe)(PPh_3)_2$, *trans*-$Ir(CO)(OMe)[P(p\text{-tolyl})_3]_2$, *trans*-$Ir(CO)(Cl)(PCy_3)_2$, and *trans*-$Ir(CO)(Me)(PCy_3)_2$, were prepared as previously described.[16] Characterization data are given in Table S1 (supplementary material).

(a) $Ir(CO)(Cl)(SO_2)[P(p\text{-tolyl})_3]_2$. In the glovebox, a saturated solution of *trans*-$Ir(CO)(Cl)[P(p\text{-tolyl})_3]_2$ in toluene-d_8 was prepared in an NMR tube equipped with a vacuum adapter. The tube was sealed under an SO_2 atmosphere on a vacuum line, and a bright green solution resulted. ^1H NMR (C_7D_8): 2.1 (s) and 7.0–8.0 (m) ppm (*p*-tolyl group). ^{31}P NMR (C_7D_8): 10.3 (s) ppm. The complex can also be prepared in a Schlenk flask in toluene solution. IR: ν_{CO} = 2015 cm^{-1}.

(b) $Ir(CO)(Cl)(SO_2)(PPh_3)_2$. In the glovebox, 0.090 g of *trans*-$Ir(CO)(Cl)(PPh_3)_2$ was suspended in 20 mL of cyclohexane in a Schlenk flask. The flask was sealed, removed from the box, and placed under an SO_2 atmosphere for 15 min. A green powder was quantitatively recovered via vacuum filtration. IR (KBr): ν_{CO} = 2013 cm^{-1}, ν_{SO} = 1197, 1049 cm^{-1}. The infrared data are consistent with those previously reported.[17]

(c) $Ir(CO)(Me)(SO_2)[P(p\text{-tolyl})_3]_2$. (i) In the glovebox, a saturated solution of *trans*-$Ir(CO)(Me)[P(p\text{-tolyl})_3]_2$ in toluene-d_8 was prepared in an NMR tube equipped with a vacuum adapter. The tube was sealed under an SO_2 atmosphere on a vacuum line, resulting in a bright green solution. ^1H NMR (C_7D_8): 1.35 (t, $J_{P\text{-}H}$ = 9.2 Hz, Ir–Me), 2.1 (s, tolyl Me), 7.0–7.9 ppm (m, tolyl). ^{31}P NMR (C_7D_8): 11.6 ppm (s). (ii) In the glovebox, 0.256 g of *trans*-$Ir(CO)(Me)[P(p\text{-tolyl})_3]_2$ was suspended in 40 mL of cyclohexane in a Schlenk flask. The flask was sealed, removed from the box, and placed under an SO_2 atmosphere. A green solution, followed by a green precipitate, formed. The solution was stirred for 1 h. The green powder was filtered off, brought into the box, and recrystallized by slow diffusion of hexane into a saturated benzene solution (yield: 0.17 g, 61.7%). IR(KBr): ν_{CO} = 2000 cm^{-1}, ν_{SO} = 1176, 1033 cm^{-1}.

(d) $Ir(CO)[OS(O)OMe](SO_2)(PPh_3)_2$. In the glovebox, a saturated solution of *trans*-$Ir(CO)(OMe)(PPh_3)_2$ in toluene-d_8 was prepared in an NMR tube equipped with a vacuum adapter. The tube was removed from the box and flame-sealed on the vacuum line under an SO_2 atmosphere. ^1H NMR: 2.6 (s, OMe), 6.8–8.0 ppm (m, phenyl). ^{31}P NMR: 14.7 (s, major), 11.6 ppm (s, minor). After 2 weeks, bright green crystals had formed in the bottom of the tube and a pale yellow solution resulted. The crystals were collected and characterized by infrared spectroscopy and a single-crystal X-ray diffraction study (vide infra). IR (KBr): ν_{CO} = 2006 cm^{-1}, ν_{SO} = 1209, 1134, 1053, 929 cm^{-1}. These crystals were found to be insoluble in toluene and became a yellow powder after sitting in toluene-d_8 for 7 days. This yellow powder was characterized by its infrared spectrum. Ir (KBr): ν_{CO} = 2046 cm^{-1}, ν_{SO} = 1226, 1190, 1118, 999 cm^{-1}.

Collection of X-ray Diffraction Data for $Ir(CO)[OS(O)OMe](SO_2)(PPh_3)_2{\cdot}0.5(toluene)$. A single crystal (dimensions 0.3 × 0.3 × 0.5 mm) was selected for the X-ray diffraction study. It was mounted in a 0.3 mm diameter thin-walled glass capillary and aligned on a Siemens R3m/V diffractometer with its extended direction essentially collinear with the instrumental ϕ axis.

---

(9) Fettinger, J. C.; Churchill, M. R.; Bernard, K. A.; Atwood, J. D. *J. Organomet. Chem.* **1988**, *340*, 377.

(10) LaPlaca, S. J.; Ibers, J. A. *Inorg. Chem.* **1970**, *9*, 1105.

(11) Vaska, L., *Acc. Chem. Res.* **1968**, *1*, 335.

(12) Levison, J. J.; Robinson, S. D. *J. Chem. Soc., Dalton Trans.* **1972**, 2013.

(13) Bell, L. K.; Mingos, D. M. P. *J. Chem. Soc., Dalton Trans.* **1982**, 673.

(14) Moroni, E. C.; Friedel, R. A.; Wender, I. *J. Organomet. Chem.* **1970**, *21*, P23.

(15) Valentine, J.; Valentine, D., Jr.; Collman, J. P. *Inorg. Chem.* **1971**, *10*, 219.

(16) (a) Randall, S. L.; Thompson, J. S.; Buttrey, L. A.; Ziller, J. W.; Churchill, M. R.; Atwood, J. D. *Organometallics* **1991**, *10*, 683 and references therein. (b) Lawson, H. J.; Atwood, J. D. *J. Am. Chem. Soc.* **1989**, *111*, 6223.

(17) Vaska, L.; Bath, S. S. *J. Am. Chem. Soc.* **1966**, *88*, 1333.

Table 1. Structure Determination Summary

empirical formula	$C_{41.5}H_{37}IrO_6P_2S_2$
color; habit	green; crystal
crystal size	0.3 × 0.3 × 0.5 mm
crystal system	triclinic
space group	$P\bar{1}$
unit cell dimens	$a = 10.972(5)$ Å $b = 11.658(4)$ Å $c = 18.020(11)$ Å $\alpha = 82.73(4)°$ $\beta = 77.76(4)°$ $\gamma = 63.25(3)°$
V	2007.5(17) Å^3
Z	2
fw	950.0
D(calc)	1.572 Mg/m^3
abs coeff	3.534 mm^{-1}
min/max transm	0.2645/0.3128
radiation	Mo Kα (λ = 0.710 73 Å)
T	297 K
no. of indep reflns	5280
no. of reflns $>6\sigma$	4502
final R indices (all data)	$R = 3.05\%$, $R_w = 3.58\%$
R indices (6σ data)	$R = 2.31\%$, $R_w = 3.23\%$

Crystal alignment and data collection were carried out as described previously;[18] details appear in Table 1. The crystal belongs to the triclinic system. Possible space groups are $P1$ and $P\bar{1}$. The latter, centrosymmetric possibility was selected as a result of intensity statistics; this choice was confirmed by the satisfactory elucidation of the structure in this higher-symmetry group. All data were corrected for Lorentz and polarization factors and for the effects of absorption.

Solution and Refinement of the Structure. All crystallographic calculations were performed with use of the Siemens SHELXTL PLUS program package.[19] The analytical scattering factors for the neutral atoms were corrected for both the real and the imaginary components of anomalous dispersion.[20] The structure was solved by a combination of direct methods and difference-Fourier syntheses. Refinement of parameters was achieved by minimization of $\sum w(|F_o| - |F_c|)^2$. All non-hydrogen atoms were located, and convergence was reached with $R = 3.05\%$, $R_w = 3.58\%$, and GOF = 0.83 for all 5280 reflections ($R = 2.31\%$ and $R_w = 3.23\%$ for those 4502 reflections with $|F_o| > 6\sigma(F_o)$). All hydrogen atoms were included in calculated positions with d(C–H) = 0.96 Å.[21] A final difference-Fourier synthesis showed no unexpected features. (The largest peak of height 1.28 e/Å^3 is close to the position of the iridium atom; the lowest trough is at −0.37 e/Å^3.) Final atomic coordinates are collected in Table 2.

Reactions. Low-temperature NMR studies were conducted as described below for *trans*-Ir(CO)(Cl)[P(p-tolyl)$_3$]$_2$ with SO_2.

In the glovebox, a saturated solution of *trans*-Ir(CO)(Cl)[P(p-tolyl)$_3$]$_2$ in CD_2Cl_2 was prepared in an NMR tube equipped with a vacuum adapter. The tube was removed from the box and flame-sealed under an SO_2 atmosphere on the vacuum line. The ^1H and ^{31}P NMR spectra were monitored as the frozen solution was warmed to room temperature. The SO_2 adduct was formed immediately at −70 °C. No change in the spectra was observed as the solution warmed, other than a sharpening of the phenyl region. ^1H NMR: 2.4 (s), 7.2–8.0 ppm (m). ^{31}P NMR: 10.1 ppm (s).

Equilibrium Studies. Equilibrium constants for SO_2 binding were evaluated for several square planar iridium complexes. Approximately 30 mg of iridium complex was placed in a jacketed reaction flask and dissolved in 25 mL of toluene. An initial infrared spectrum was recorded to accurately measure the concentration by comparison to a Beer's law plot. The flask was placed under a gas mixture containing SO_2 and then heated to 56.5 °C by a constant-temperature circulator (Haake). After 1 h, the infrared spectrum was recorded and the concentration of the square planar complex evaluated from the absorbance. The concentration of SO_2 adduct was evaluated from integrated areas of the infrared spectrum. SO_2 concentrations were evaluated by using SO_2 solubility data at 60 °C.[22] The equilibrium constants evaluated are given in Table 3. Error limits are quoted as standard deviations.

Table 2. Atomic Coordinates (×10^4) and Equivalent Isotropic Displacement Coefficients (Å^2 × 10^3)

	x	y	z	U(eq)[a]
Ir(1)	276(1)	2357(1)	2319(1)	35(1)
P(1)	2214(1)	1199(1)	1393(1)	38(1)
P(2)	−1638(1)	3840(1)	3151(1)	41(1)
S(1)	−47(2)	514(1)	2975(1)	57(1)
O(11)	−1127(5)	436(4)	2684(3)	103(3)
O(12)	1277(4)	−578(4)	2812(3)	75(2)
S(2)	2420(1)	2818(1)	3050(1)	53(1)
O(21)	1430(4)	3714(4)	3780(2)	69(2)
O(22)	2217(4)	3684(4)	2383(2)	62(2)
O(23)	1568(4)	2065(3)	3088(2)	51(2)
C(1)	−807(6)	2661(5)	1603(3)	47(2)
O(1)	−1454(4)	2862(4)	1138(2)	68(2)
C(2)	1896(9)	4583(7)	3958(4)	93(5)
C(11)	2354(6)	−270(5)	1029(3)	47(2)
C(12)	3618(6)	−1276(5)	818(3)	55(3)
C(13)	3714(7)	−2347(6)	526(3)	72(3)
C(14)	2554(9)	−2429(6)	442(4)	85(4)
C(15)	1270(8)	−1429(7)	648(4)	92(5)
C(16)	1168(7)	−351(6)	950(4)	71(3)
C(21)	3897(5)	707(5)	1668(3)	44(2)
C(22)	4816(6)	1176(5)	1300(3)	54(3)
C(23)	6056(6)	810(6)	1548(4)	64(3)
C(24)	6378(6)	−28(6)	2150(4)	73(3)
C(25)	5472(7)	−514(6)	2520(4)	67(3)
C(26)	4220(6)	−156(5)	2288(3)	53(3)
C(31)	2191(5)	2256(5)	543(3)	43(2)
C(32)	1900(6)	3515(5)	639(3)	55(3)
C(33)	1874(7)	4336(6)	14(3)	66(3)
C(34)	2145(7)	3908(6)	−703(3)	71(3)
C(35)	2429(7)	2674(6)	−801(3)	76(3)
C(36)	2454(6)	1830(5)	−177(3)	58(3)
C(41)	−3275(5)	4443(5)	2814(3)	45(2)
C(42)	−3719(6)	3570(6)	2646(3)	62(3)
C(43)	−4935(6)	3986(6)	2382(4)	75(4)
C(44)	−5736(7)	5272(7)	2261(4)	75(3)
C(45)	−5321(6)	6153(6)	2416(3)	64(3)
C(46)	−4091(6)	5732(5)	2689(3)	53(3)
C(51)	−1990(6)	3281(5)	4132(3)	51(3)
C(52)	−884(7)	2536(7)	4508(3)	69(3)
C(53)	−1165(8)	2165(8)	5270(3)	87(4)
C(54)	−2483(8)	2505(7)	5642(3)	85(4)
C(55)	−3563(8)	3200(7)	5276(4)	100(4)
C(56)	−3339(7)	3600(6)	4510(4)	81(3)
C(61)	−1450(6)	5281(5)	3235(3)	48(2)
C(62)	−814(6)	5754(5)	2610(3)	57(3)
C(63)	−672(7)	6875(6)	2653(4)	75(4)
C(64)	−1205(9)	7519(6)	3315(5)	92(5)
C(65)	−1875(9)	7085(7)	3946(5)	100(5)
C(66)	−2000(7)	5952(6)	3910(4)	71(3)
C(71)	4455	519	4456	115(3)
C(72)	3393	230	4469	109(5)
C(73)	3243	−372	5318	183(5)
C(74)	4180	−781	5806	100(5)
C(75)	5502	204	4786	129(7)

[a] Equivalent isotropic U defined as one-third of the trace of the orthogonalized $\mathbf{U}_{ij}$ tensor.

Results and Discussion

Binding of SO_2 to *trans*-Ir(CO)(Cl)(PPh$_3$)$_2$ has been previously reported[17] and the crystal structure deter-

---

(18) Churchill, M. R.; Lashewycz, R. A.; Rotella, F. J. *Inorg. Chem.* **1977**, *16*, 265.

(19) *Siemens SHELXTL PLUS Manual*, 2nd ed.; Siemens Analytical Instruments: Madison, WI, 1990.

(20) *International Tables for X-ray Crystallography*; Kynoch Press: Birmingham, England, 1974; Vol. 4, pp 99–101, 149–150.

(21) Churchill, M. R. *Inorg. Chem.* **1973**, *12*, 1213.

(22) Lloyd, S. J. *J. Phys. Chem.* **1918**, *22*, 300. For L = PCy$_3$, the equilibrium constants were evaluated in C_6H_{12} using the SO_2 solubility data for toluene.

Table 3. Equilibrium Constants for SO_2 Complexes of Iridium(I)

complex	adduct	K_{eq} (L/mol)
$Ir(CO)(Cl)[P(p\text{-tolyl})_2]_2$	$Ir(CO)_2(Cl)(SO_2)[P(p\text{-tolyl})_3]_2$	1400 ± 700
$Ir(CO)(CH_3)[P(p\text{-tolyl})_3]_2$	$Ir(CO)(CH_3)(SO_2)[P(p\text{-tolyl})_3]_2$	not reversible
$Ir(CO)(Cl)(PCy_3)_2$	$Ir(CO)(Cl)(SO_2)(PCy_3)_2$	5.24 ± 0.17
$Ir(CO)(CH_3)(PCy_3)_2$	$Ir(CO)(CH_3)(SO_2)(PCy_3)_2$	1600 ± 200
$Ir(CO)(Cl)(PPh_3)_2$	$Ir(CO)(Cl)(SO_2)(PPh_3)_2$	1200 ± 100
$IrBr(CO)[P(p\text{-tolyl})_3]_2$	$IrBr(CO)(SO_2)[P(p\text{-tolyl})_3]_2$	1300 ± 800

mined.[10] Similar reactions are observed for $Ir(CO)L_2X$ (X = Cl, Br, Me; L = PPh_3, $P(p\text{-tolyl})_3$, PCy_3).

$$Ir(CO)(Cl)L_2 + SO_2 \xrightarrow[\text{1 atm}]{\text{room temp}} Ir(CO)(Cl)(SO_2)L_2 \quad (6)$$

$$L = PPh_3,\ P(p\text{-tolyl})_3$$

$$Ir(CO)(Me)L_2 + SO_2 \xrightarrow[\text{1 atm}]{\text{room temp}} Ir(CO)(Me)(SO_2)L_2 \quad (7)$$

$$L = P(p\text{-tolyl})_3$$

Sulfur dioxide insertion into metal–methyl bonds has previously been observed.[23] Two pieces of data indicate that insertion of SO_2 into the Ir–Me bond does not occur: (1) Coupling of the phosphorus nuclei to the methyl is observed in the SO_2 adducts and (2) The ν_{SO} values of 1176 and 1033 cm^{-1} for $Ir(CO)(Me)(SO_2)[P(p\text{-tolyl})_3]_2$ are very similar to those for $Ir(CO)(Cl)(SO_2)(PPh_3)_2$, 1197 and 1049 cm^{-1}. Both are consistent with SO_2 bound to iridium through the sulfur atom.[2] The change in the carbonyl stretching absorption to higher frequency indicates that the SO_2 is functioning as a Lewis acid and removing electron density from the iridium.

At higher temperatures, the SO_2 binding is an equilibrium for some chloro complexes with different phosphine ligands. Values for several complexes at 56.5 °C are shown in Table 3. The methyl complexes bind SO_2 tightly such that even at 56.5 °C only the SO_2 adduct is observed in solution. This would be expected since CH_3 is a substantially better donor and the enhanced electron density on iridium creates a stronger bond to SO_2. This emphasizes that the iridium is a donor to SO_2. The values for the equilibrium constants show that steric interactions inhibit SO_2 binding since the equilibrium constant for the very large, strong donor PCy_3 complex is 2 orders of magnitude less than for the PPh_3 and $P(p\text{-tolyl})_3$ complexes. The binding of SO_2 may be compared to the binding of other gases to Ir(I) square planar complexes

$$O_2,\ H_2 > SO_2 > CO > CO_2$$

because O_2 and H_2 are essentially irreversibly bound and CO_2 does not show any evidence for an adduct. A competitive experiment shows the CO equilibrium constant to be about half that for SO_2 in reaction with *trans*-$Ir(CO)(Cl)[P(p\text{-tolyl})_3]_2$.[24] This order is consistent with the binding order previously determined.[11] The bindings of O_2 and H_2 are oxidative addition reactions resulting in Ir(III) complexes. For the simple Ir(I) adducts, SO_2 is the most strongly bound of the gases examined.

To further examine the binding of SO_2, several of the iridium(I) complexes were treated with mixtures of SO_2 in air (see eqs 8–11). The products depend on the nature

$$Ir(CO)(Cl)L_2 + SO_2\ (936\ \text{ppm in air}) \overset{25\ °C}{\rightleftarrows} Ir(CO)(Cl)(SO_2)L_2 \quad (8)$$

$$Ir(CO)(Cl)L_2 + SO_2\ (103\ \text{ppm in air}) \xrightarrow{25\ °C} Ir(CO)(Cl)(O_2)L_2 \quad (9)$$

$$Ir(CO)(Me)L_2 + SO_2\ (1.1\%\ \text{or}\ 11\,000\ \text{ppm in air}) \xrightarrow{25\ °C} Ir(CO)(Me)(SO_4)L_2 \quad (10)$$

$$Ir(CO)(Me)L_2 + SO_2\ (103\ \text{ppm in air}) \xrightarrow{25\ °C} Ir(CO)(Me)(O_2)L_2 \quad (11)$$

$$L = P(p\text{-tolyl})_3$$

of the X group in *trans*-$Ir(CO)[P(p\text{-tolyl})_3]_2X$ and on the concentration of SO_2. The reactions of the chloro complex show that the binding of SO_2 is kinetically favored over that of O_2, since the SO_2 adduct is formed in reaction 8. The reaction products are those obtained after 1 h; only the methyl complex with 1.1% SO_2 in air results in the formation of the sulfate complex (see eq 10). Reaction of the chloro complex with SO_2 and O_2 results in the formation of sulfate overnight.[15] Reactions of the chloro complex, *trans*-$Ir(CO)(Cl)[P(p\text{-tolyl})_3]_2$, with an SO_2–air mixture illustrate the relative binding of O_2 and SO_2. For 1.1% SO_2 in air after 1 h at room temperature, only the SO_2 adduct (ν_{CO} = 2015 cm^{-1}) is observed. Even though O_2 is present at 25 times the amount of SO_2, SO_2 is preferentially bound. After 24 h, about 15% is converted to the sulfate complex (2043 cm^{-1}) but the SO_2 adduct is still dominant and the O_2 adduct is less than 5%. For a 103 ppm SO_2 mixture in air after 1 h, the O_2 adduct is formed with about 20% of the SO_2 adduct. After 24 h, formation of the O_2 adduct has continued, but the SO_2 adduct is decreased. Some sulfate complex is observed (~10%). The O_2 adduct is formed much more slowly than the SO_2 adduct but, once formed, does not lose O_2 at room temperature.

Sulfur Dioxide Insertion. Reaction of SO_2 with the methoxy complexes, *trans*-$Ir(CO)(OMe)L_2$ (L = PPh_3, $P(p\text{-tolyl})_3$), proceeds from the yellow iridium(I) complex to the usual green solution from which green crystals may be separated. The characterization of these green complexes is relatively similar to the characterization of the SO_2 adducts of the chloro and methyl complexes except for the presence of additional S–O stretching absorptions in the infrared spectrum. To better understand these products of the reaction of SO_2 with the methoxy com-

---

(23) Vitzthum, G.; Lindner, E. *Angew. Chem., Int. Ed. Engl.* **1971**, *10*, 315 and references therein.

(24) For evaluation of the CO equilibrium constant, a competition with SO_2 was established.

$$K_{eq} = \frac{[IrSO_2]_{eq}[CO]_{eq}}{[IrCO]_{eq}[SO_2]_{eq}} = \frac{K_{SO_2}}{K_{CO}}$$

The [CO] was determined from data in the literature (at 330 K, $\chi_2 = 8.94 \times 10^4$ mol of CO/mol of solution).[25] The concentration of $IrCl(CO)_2[P(p\text{-tolyl})_3]_2$ was determined from a Beer's law plot, and that of $Ir(CO)(Cl)(SO_2)[P(p\text{-tolyl})_3]_2$, by difference from the initial.

(25) Field, L. R.; Wilhelm, E.; Battino, R. *J. Chem. Thermodyn.* **1974**, *6*, 237.

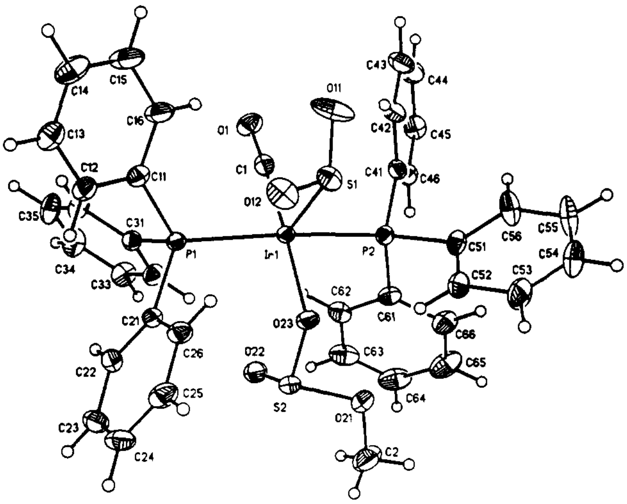

Figure 1. ORTEP diagram for Ir(CO)(OS(O)OMe)$(PPh_3)_2$ showing the atomic labeling.

Table 4. Selected Interatomic Distances (Å) and Angles (deg) for Ir(CO)[OS(O)OMe]$(SO_2)(PPh_3)_2$·0.5(toluene)

(A) Iridium–Ligand Distances			
Ir(1)–P(1)	2.369(2)	Ir(1)–O(23)	2.080(4)
Ir(1)–P(2)	2.387(2)	Ir(1)–C(1)	1.831(6)
Ir(1)–S(1)	2.451(2)	C(1)–O(1)	1.147(8)
(B) Distances in Ir(SO_2) Systems			
S(1)–O(11)	1.435(7)	S(1)–O(12)	1.437(4)
(C) Distances within Ir[OS(O)OMe] Systems			
S(2)–O(21)	1.650(4)	S(2)–O(23)	1.531(5)
S(2)–O(22)	1.456(4)	O(21)–C(2)	1.417(12)
(D) Angles around the Iridium Atom			
P(1)–Ir(1)–P(2)	170.3(1)	P(1)–Ir(1)–S(1)	97.5(1)
P(2)–Ir(1)–S(1)	92.2(1)	P(1)–Ir(1)–O(23)	90.8(1)
P(2)–Ir(1)–O(23)	89.9(1)	S(1)–Ir(1)–O(23)	85.8(1)
P(1)–Ir(1)–C(1)	87.5(1)	P(2)–Ir(1)–C(1)	91.4(1)
S(1)–Ir(1)–C(1)	97.3(2)	O(23)–Ir(1)–C(1)	176.7(2)
(E) Angles Involving the SO_2 Ligand			
Ir(1)–S(1)–O(11)	106.9(2)	O(11)–S(1)–O(12)	113.8(3)
Ir(1)–S(1)–O(12)	105.5(2)		
(F) Angles within Ir[OS(O)OMe] Systems			
Ir(1)–O(23)–S(2)	123.5(2)	O(22)–S(2)–O(23)	108.8(3)
O(21)–S(2)–O(22)	106.0(2)	S(2)–O(21)–C(2)	114.0(4)
O(21)–S(2)–O(23)	95.4(2)		

plexes, the structure was determined for the product of the reaction of SO_2 with *trans*-Ir(CO)(OMe)$(PPh_3)_2$.

The crystal consists of ordered molecular units of Ir(CO)[OS(O)OMe]$(SO_2)(PPh_3)_2$ and disordered toluene molecules (defined by atoms C(71)–C(75) and the related atoms and disposed about the inversion center at $^1/_2$, 0, $^1/_2$) in a 1:0.5 ratio. The entire iridium complex is illustrated in Figure 1. Interatomic distances and angles are collected in Tables S2 and S3 (supplementary material). Selected distances and angles are shown in Table 4. The iridium complex is extremely unusual insofar as it has incorporated two sulfur dioxide moieties into the structure—the first as a simple S-bonded η^1-SO_2 ligand and the second into an Ir–OCH_3 linkage, producing an Ir—O—S(=O)—OCH_3 system.

The iridium(I) atom has a square pyramidal coordination environment, with the S-bonded SO_2 ligand occupying the apical site. The iridium–sulfur distance is Ir(1)–S(1) = 2.451(2) Å, with S(1)–O(11) = 1.435(7) Å and S(1)–O(12) = 1.437(4) Å; the pyramidal geometry about S(1) is indicated by the small (all <120°) angles about S(1), with Ir(1)–S(1)–O(11) = 106.9(2)°, Ir(1)–S(1)–O(12) = 105.5(2)°, and O(11)–S(1)–O(12) = 113.8(3)°.

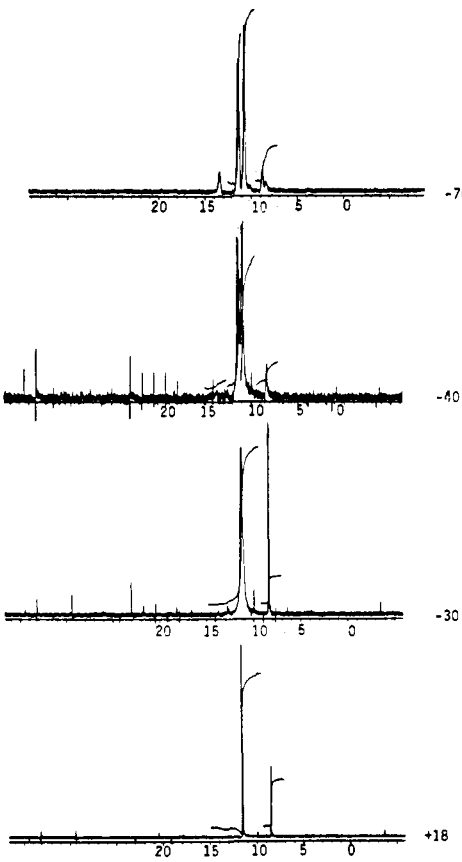

Figure 2. Variable-temperature ^{31}P NMR spectra of *trans*-Ir(CO)(OMe)[P(*p*-tolyl)$_3$]$_2$ under an SO_2 atmosphere.

Angles from the basal ligands to the apical ligand are all in the range 85–98°, with (in increasing order) O(23)–Ir(1)–S(1) = 85.8(1)°, P(2)–Ir(1)–S(1) = 92.2(1)°, C(1)–Ir(1)–S(1) = 97.3(2)°, and P(1)–Ir(1)–S(1) = 97.5(1)°.

The iridium–ligand distances in the basal plane are Ir(1)–P(1) = 2.369(2) Å, Ir(1)–P(2) = 2.387(2) Å, Ir(1)–C(1) = 1.831(6) Å, and Ir(1)–O(23) = 2.080(4) Å. The two phosphine ligands are trans to one another (P(1)–Ir(1)–P(2) = 170.3(1)°) as are the carbonyl and methyl sulfite ligands (C(1)–Ir(1)–O(23) = 176.7(2)°).

The most unusual portion of the molecule is that involving the methyl sulfito ligand. Distances within the IrOS(=O)OCH_3 systems are as follows: Ir(1)–O(23) = 2.080(4) Å, S(2)–O(22) = 1.456(4) Å (presumably an S=O double bond), S(2)–O(23) = 1.531(5) Å, S(2)–O(21) = 1.650(4) Å, and O(21)–C(2) = 1.417(12) Å. Atom S(2) is formally a sulfur(IV) species and has a pyramidal geometry with O(21)–S(2)–O(22) = 106.0(2)°, O(21)–S(2)–O(23) = 95.4(2)°, and O(22)–S(2)–O(23) = 108.8(3)°. This sulfur atom has three different groups attached to it, is a site of C_1 symmetry, and is thus a chiral center. [Note that the crystal crystallizes in space group $P\bar{1}$; the "other" molecule in the unit cell consists of the reverse enantiomer.] The SO_2 moiety inserted into the Ir–OMe bond (1134 and 929 cm^{-1}) and a second coordinated SO_2 ligand (1209 and 1053 cm^{-1}) account for the S–O stretching absorptions.

Low-temperature NMR spectra of the P(*p*-tolyl)$_3$ complex under an atmosphere of SO_2 (Figure 2) show only a second-order spectrum, indicating two inequivalent phosphine ligands. This is assigned to Ir(CO)[OS(O)OMe](SO_2)[P(*p*-tolyl)$_3$]$_2$, where the asymmetry derives from the chiral center at S(2), a pyramidally coordinated sulfur(IV) atom formed by insertion of SO_2 into the Ir–OMe ligand. As the temperature is increased, two changes occur. (1) Inversion of the sulfur center occurs, causing broadening and finally coalescence of the ^{31}P resonance for Ir(CO)[OS(O)OMe](SO_2)[P(*p*-tolyl)$_3$]$_2$ to the room-temperature resonance of 11.5 ppm as the temperature changes from −70 to 0 °C. (2) A new singlet is formed at 8.4 ppm that appears to be due to the rearrangement product (see below). Cooling the NMR tube back to −70 °C causes the resonance from Ir(CO)[OS(O)OMe](SO_2)[P(*p*-tolyl)$_3$]$_2$ to regenerate the second-order spectrum but does not affect the 8.4 ppm (s) resonance. Upon being stored in solution, the complex rearranges to a product with ν_{CO} = 2046 cm^{-1}, $\delta(^1H)$ = 2.7 ppm (s, methyl on the OSO_2Me ligand), and $\delta(^{31}P)$ = 8.4 ppm (s). This species does not have the green color of pyramidal SO_2 adducts, does not evolve SO_2, and does not react with O_2. We tentatively assign this product as Ir(CO)(SO_2OMe)(SO_2)L_2, where the oxygen-coordinated methyl sulfito ligand has rearranged to the sulfur-coordinated ligand and the SO_2 is now coplanar. Factors important to pyramidal versus coplanar SO_2 have been discussed.[26] The S–O stretches for the yellow product at 1226 and 1118 cm^{-1} indicate a coplanar SO_2 ligand, and the other two at 1190 and 999 cm^{-1} are consistent with a sulfur-coordinated methyl sulfito ligand. Rearrangement of the oxygen-coordinated to a sulfur-coordinated methyl sulfito ligand would also remove the asymmetric center, consistent with the unchanged ^{31}P NMR resonance at 8.4 ppm as the temperature is cooled. Although never before structurally characterized, the oxygen-coordinated methyl sulfito ligand has been suggested as an intermediate in SO_2 insertion reactions that result in sulfur-coordinated methyl sulfite.

Very similar reaction sequences are observed for Ir(CO)(*t*-BuO)(PPh_3)$_2$. A second-order spectrum, similar to that observed for the methoxy analogue shown in Figure 2, is attributed to Ir(CO)[OS(O)O-*t*-Bu](PPh_3)$_2$, with inversion at the sulfur occurring similarly to that of the methoxy complex. In this case, the sulfinato-*S* product forms at −70 °C, as opposed to −40 °C for the methoxy analogue.

A previous report of SO_2 insertion into iridium–oxygen bonds assigned the product as the sulfur-coordinated sulfinate.[27] On the basis of the similarity of infrared absorptions to those reported herein for the oxygen-coordinated sulfito complexes, it is likely that the oxygen-coordinated sulfite was formed.

Reaction of *trans*-Ir(CO)(OH)L_2 with SO_2 is similar to reactions of the methoxo and *tert*-butoxo analogs only at low temperature in solution or at room temperature in the solid state. At room temperature, reaction in solution proceeds through a green intermediate to a yellow solution for which the ^{31}P NMR spectrum is quite complicated (Figure 3). Low-temperature addition of SO_2 for the P(*p*-tolyl)$_3$ complex results in a broad ^{31}P resonance at 9.1 ppm which sharpens and shifts to 13.5 ppm as the temperature increases. This is the major peak and is presumed to be due to the hydrogen sulfite species, Ir(CO)[OS(O)OH](SO_2)L_2, by analogy to the previously discussed reactions. A singlet appears at 8.0 ppm as the solution is warmed. This minor peak is tentatively assigned to the sulfinato-*S*, coplanar SO_2 product, Ir(CO)(SO_3H)(SO_2)L_2. A small unassigned singlet at 9.6 ppm is unchanged from −70 °C to +18 °C. The green product, Ir(CO)[OS(O)OH](SO_2)L_2, could also be prepared by reaction in the solid state. For L = PPh_3, this product has a ν_{CO} at 2004 cm^{-1} with the pyramidal SO_2 ligand having ν_{SO} at 1213 and 1053 cm^{-1} and the hydrogen sulfito ligand having ν_{SO} at 1072 and 918 cm^{-1}. These values are close to those of the structurally characterized methoxy analog. This green product turns yellow upon exposure to air for several days. The yellow product had ν_{CO} at 2042 cm^{-1} and ν_{SO} at 1172 and 1120 cm^{-1}. The ν_{SO} at 1120 cm^{-1} is assigned to a coplanar SO_2 ligand, and the ν_{SO} at 1172 cm^{-1} is assigned to the sulfinato-*S* ligand. These values are close to those found for the previously described sulfinato-*S* products; however the additional ν_{SO} bands were not observed.

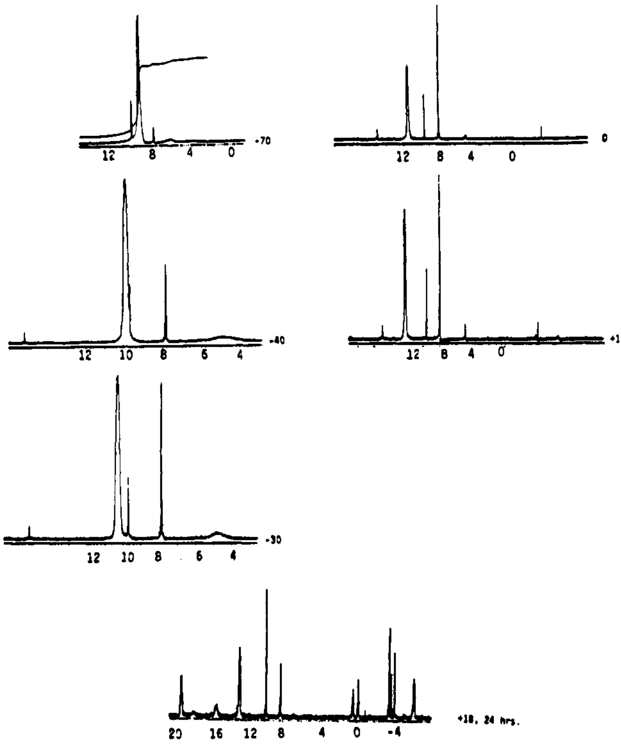

Figure 3. Variable-temperature ^{31}P NMR spectra of *trans*-Ir(CO)(OH)[P(*p*-tolyl)$_3$]$_2$ under an SO_2 atmosphere.

The addition of SO_2 at room temperature produces a ^{31}P NMR spectrum that indicates several products. For the P(*p*-tolyl)$_3$ complex, a ^{31}P resonance at 19.1 ppm is always similar in intensity to a −6.5 ppm resonance, suggesting that they are related. The resonance at −6.5 ppm may be assigned to free P(*p*-tolyl)$_3$. Because the resonance at 19.1 ppm is within the region of four-coordinate iridium(I), one may postulate that this resonance is due to a four-coördinate species produced as a result of phosphine loss from a more highly coordinated metal center. In addition to these resonances, four doublets are present that arise from second-order coupling. The two inequivalent phosphines have resonances at 1.64 and −2.72 ppm, with a coupling constant of 92 Hz. The magnitude of the coupling constant suggests cis phosphines. In addition, the second-order spectrum is split into a series of doublets with a coupling constant of 10.0 Hz. The magnitude of this coupling constant suggests proton–phosphorus coupling. A potential source of a hydrido ligand would be deprotonation of the HSO_3^- ligand, resulting in a hydrido ligand as well as an SO_3^{2-}

---

(26) Reinhold, J.; Schuler, M.; Hoffman, T.; Wenschuh, E. *Inorg. Chem.* **1992**, *31*, 559.
(27) Green, L. M.; Meek, D. W. *Organometallics* **1989**, *8*, 659.

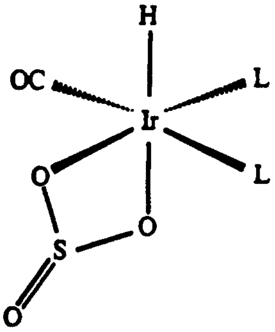

Figure 4. Suggested decomposition product from reaction of SO_2 with *trans*-Ir(CO)(OH)[P(*p*-tolyl)$_3$]$_2$.

ligand. These data then suggest the product shown in Figure 4. Loss of H^+ from an HSO_3^- ligand has been reported in the literature.[3]

$$Cp^*Ru(CO)_2SO_3H + NEt_3 \rightarrow [Et_3NH]^+[Cp^*Ru(CO)_2SO_3]^- \quad (12)$$

$$Cp^*Ru(CO)_2SO_3H + CH_3OH \rightarrow Cp^*Ru(CO)_2SO_3CH_3 + H_2O \quad (13)$$

$$CpFe(CO)_2SO_3H + NaOH \rightarrow Na^+[CpFe(CO)_2SO_3]^- + H_2O \quad (14)$$

The above examples consist of coordinatively saturated metal complexes. In the case of $Ir(CO)(SO_3H)(SO_2)L_2$, an open coordination site exists for H^+ to bind.

It thus seems that there are two pathways available through which $Ir(CO)(SO_3H)(SO_2)L_2$ can decompose. One involves desulfination of the sulfinato ligand, forming free phosphine and a four-coordinate iridium complex, possibly $HOIr(CO)(SO_2)L$. The second route involves proton loss from the HSO_3^- ligand to form the iridium(III) complex $HIr(CO)(SO_3)L_2$.

The reaction of $HIr(CO)(PPh_3)_3$ with SO_2 has been previously reported in the literature:[12]

$$HIr(CO)(PPh_3)_3 + SO_2 \rightarrow HIr(CO)(SO_2)(PPh_3)_2 + PPh_3 \rightleftharpoons HSO_2Ir(CO)(PPh_3)_2 + PPh_3 \quad (15)$$

However, the report of a rapid tautomerism in the hydrido–SO_2 complex could not be substantiated.[13] To clarify these conflicting reports, the reactivity of HIr(CO)[P(*p*-tolyl)$_3$]$_3$ with SO_2 was examined . The hydrido–SO_2 complex as well as the inserted product could be observed using ^1H and ^{31}P NMR. The hydrido–SO_2 complex was identified as the major species in solution, with a ^{31}P resonance at 16.6 ppm and a triplet at −2.7 ppm in the ^1H NMR spectrum due to the hydrido ligand. The triplet in the ^1H spectrum has been previously reported.[13] The inserted product was formed to a lesser extent and was characterized by its ^{31}P resonance at 20.3 ppm and ^1H resonance at 4.5 ppm (s) due to the hydrogen sulfinato ligand. By comparison to previous work, the 4.5 ppm resonance is most consistent with an O–H bond.[5] Free phosphine was also observed in the ^{31}P NMR spectrum.

Sulfur Dioxide Binding. The binding of SO_2 and reaction chemistry of SO_2 coordinated to a metal are of tremendous importance for improving the technology of SO_2 removal. Reactions of SO_2 with square planar iridium complexes have shown the following: (1) Increasing the electron density at iridium enhances the binding of SO_2. (2) Increasing the size of the phosphine ligand decreases the binding of SO_2. (3) The order for gases binding to *trans*-Ir(CO)(Cl)[P(*p*-tolyl)$_3$]$_2$ is H_2, O_2 > SO_2 > CO > CO_2, H_2O. (4) Sulfur dioxide binds to iridium(I) more rapidly than O_2. (5) Sulfur dioxide does not insert into an iridium–alkyl bond but inserts into iridium–oxygen bonds very rapidly (even at −70 °C). (6) Sulfur dioxide bound to iridium(I) in a pyramidal geometry produces a green color and may sometimes be displaced. (7) Pyramidally bound SO_2 may rearrange to coplanar, which is irreversibly bound. (8) Sulfur dioxide that is inserted into an iridium–oxygen bond cannot be deinserted.

While aspects of these observations have been previously discussed, such systematic examination of a series of related complexes provides a more comprehensive picture of sulfur dioxide binding and rearrangements.

Acknowledgment. We are grateful to the National Science Foundation (Grant CHE-9015897) for support of this research and for funding the purchase of the diffractometer (Chemical Instrumentation Program, Grant 89-13733). We also acknowledge the Department of Education (Grant 2-2-01011) for a grant that allowed the purchase of a Varian VXR-400 NMR spectrometer. S.L.R acknowledges a University at Buffalo Presidential Fellowship and an Allied-Signal Fellowship, and T.S.J. acknowledges support from the Research Corp. (Grant C 2971). Dr. Holly Lawson prepared *trans*-Ir(CO)(Me)(PCy$_3$)$_2$ and *trans*-Ir(CO)(Cl)(PCy$_3$)$_2$.

Supplementary Material Available: Tables of IR and NMR data, bond lengths, bond angles, anisotropic thermal parameters, hydrogen coordinates and isotropic thermal parameters, and details of the structure determination (8 pages). Ordering information is given on any current masthead page.

OM930536B